

Original Research

Comparative Study on Emission Reduction Performance of Two Organic Acid Rare Earth Fuel Additives for Diesel Engines

Guo Junwu*, Guo Leyang

Shanghai Maritime University, Marine Merchant College, Shanghai, No. 1550 Haigang Avenue, China

Received: 8 July 2022

Accepted: 6 December 2022

Abstract

As fuel additives, lanthanum and cerium are the most active rare earth elements. In order to compare the emission reduction performance of the two rare earth elements additives, lanthanum oxalate and cerium oxalate are used as the comparison objects in this paper. In order to reduce the error, it is necessary to prepare lanthanum oxalate and cerium oxalate. After lanthanum oxalate and cerium oxalate was prepared by precipitation method, a series of modern characterization methods, such as XRD, SEM, EDS and BET, are used to characterize and analyze the self-made additive powder, and the relationship between the emission reduction performance and the internal relationship is analyzed. By changing the ratio of fuel additives and carrying out the emission test on the self-built diesel engine platform, the optimal amount of additives is obtained. Fuel additives of lanthanum oxalate and cerium oxalate with a mass fraction of about 45mg/L for diesel engine is a more suitable choice. Cerium oxalate has better emission reduction performance than lanthanum oxalate. The conclusion is that reasonable use of two organic acid rare earth fuel additives can greatly reduce NO_x , CO and HC emissions from diesel engines.

Keywords: characterization, emission reduction, fuel additive, organic acid rare earth

Introduction

Environmental problems have become the focus of society more and more, and scholars all over the world have conducted relevant studies. In the study of Elsunousi A.A.M. et al. [1], it was aimed to determine the regional and periodic change of CO_2 and particulate matter pollution in the city of Misurata, one of the important cities of Libya.

The results of the study of Cetin M. et al. [2] showed that the effect of season on noise and CO_2 was statistically insignificant, but the particulate matter dimensions are affected at statistically 99.9% confidence level by season.

The findings of the present study of Cetin M. [3] indicated that the threshold value was usually exceeded within 10 minutes, following the start of exams, and when indoor CO_2 amounts were higher than 1500 ppm, which was considered in most exams as the limit of harm to health, and circulating air in the hallways and keeping the doors of exam halls open throughout the exam period were not adequate for keeping the indoor CO_2 amounts below 1000 ppm.

*e-mail: jwguo@shmtu.edu.cn

In the study of Cetin M. et al. [4], the particulate matter (0.3, 0.5 and 5 μm dimensions) and carbon dioxide (CO_2) amounts were measured and evaluated in Kastamonu city. Measurement results obtained from 7 regions in the Kastamonu city with different properties were evaluated and comparisons were made in terms of air quality.

The study of Cetin M. et al. [5] aimed to determine and map the Pb and Cr pollution in the city center of Ankara, the capital and the second-largest city of Turkey, with the help of topsoils.

In addition, the exhaust gas of diesel engines also has caused great harm to the environment. In order to solve the environmental pollution problem of the diesel engine exhaust gas, fuel additives can be used to clean the diesel fuel system, enhance the power performance of the fuel, eliminate black smoke and reduce emissions. At present, many scholars have studied the emission reduction performance of internal combustion engine.

Zhang C. et al. [6] based on the engine test bench, tested the addition of a small amount of iron-based fuel additives to diesel, and studied the effects of fuel additives on diesel particulate emissions from the aspects of number concentration and particle size distribution characteristics, exhaust smoke, oxidation characteristics of particulate matter and so on. Gong J. et al. [7] established a computational model for catalytic regeneration of DPF with Cerium-based additives based on the assisted regeneration model of particle trap (DPF) NO_2 and carried out experimental verification. Ji G. et al. [8] tested the emission characteristics of CeO_2 or Co_3O_4 nanoparticles mixed with diesel fuel with mass fraction of 50 mg/kg and 100 mg/kg on a 186FA diesel engine. The microstructures, morphology and thermogravimetric characteristics of the collected particles were analyzed by scanning electron microscopy and thermogravimetric analyzer. Mei D. et al. [9] used the Moudi sampler to collect diesel particulate matter, and conducted thermogravimetric analysis tests on four particle sizes of 0.18-0.32, 0.32-0.56, 0.56-1.00 and 1.00-1.80 μm in pure N_2 and O_2 environments. Song D. et al. [10] studied the influence of two kinds of fuel additives on the exhaust pollutants of diesel engines of new and old fishing boats through the bench test of propulsion characteristics, and introduced the weighting coefficient to calculate the weighted purification rate. Through comparative analysis, they provided a reference for fishermen to correctly choose fuel additives. Ma Z. et al. [11] carried out a pistacia chinesis biodiesel-diesel fuel test on a YTR3105 direct-injection diesel engine, and analyzed the economic, combustion and emission characteristics under different loads. Experimental study by Zhang D. et al. [12] showed that the nanometer CeO_2 diesel additive could save the fuel of internal combustion engine up to about 7%, and at the same time reduce the total hydrocarbons, particulate matter and other harmful substances and smoke in emissions. Wu Q. et al. [13] prepared CeO_2 -diesel mixed fuel with mass fraction of 50 mg/L

and 100 mg/L by adding micro nano CeO_2 particles into Diesel, labeled as D50C and D100C. Taking Diesel as reference, the combustion and emission performance of these three fuels were compared and studied on 186FA Diesel engine. Wang D. et al. [14] directly added a trace amount of iron based additives to low sulfur diesel, and studied the effects of iron based additives on diesel engine performance, gas emissions, particle number and concentration and particle size distribution through engine bench test. Tian J. et al. [15] added iron based fuel additive (FBC) to 0# diesel for vehicle use, and carried out the trap loading and regeneration test on a CA6DL2-35E3 high pressure common rail heavy diesel engine equipped with an uncoated silicon carbide particle trap (DPF).

In the paper of Danilov A.M. [16], the situation evolved in the domain of fuel additives production during 2011-2015 is reviewed through the analysis of literature and patent sources and statistical data. In the study of Xie Y. et al. [17], tellurium was investigated as a potential additive to metallic fuel (e.g. U-10Zr) to mitigate fuel-cladding chemical interaction (FCCI). The paper of Bennett J. [18] discusses where performance fuel additives provide their benefits and how they are evolving to work with latest generations of fuel and engines, and provides an overview of the current and upcoming industry engine tests for fuels and their additives. Larsson E. et al. [19] investigates the friction reducing properties and fuel saving potential of a boric acid based fuel additive with remarkably promising results in field tests. The effect of normal load and sliding velocity on the friction behavior was studied with a reciprocating model test developed to mimic the dual lubrication from the fuel additive and the engine oil. Substantial friction reductions were achieved when repeatedly spraying the fuel additive on base oil lubricated surfaces. The friction energy loss was reduced by up to 76% compared to references without the fuel additive. Influence of biodiesel-diesel fuel blends with acetylferrocene and palladium based additives on diesel engine performance and emissions were studied experimentally by Keskin A. et al. [20]. The main aim of the study of Akbarian E. et al. [21] is to use the blend of glycerol triacetate (GT) additive and biodiesel to reduce emissions and to improve fuel cost of dual-fuelled diesel engine by natural gas as main fuel. This study of Sezer I. [22] compiled the results of various researches performed on using nanomaterials additives in diesel engine fuels such as diesel, biodiesel, water emulsified fuels and various fuel blends.

The current research work of Rosales J. et al. [23] seeks to characterize U_3Si_2 surrogate materials fabricated by a laser synthesis. The characterization results provided novel microstructural data that aided in the early development stages of an additive manufacturing process. For this study, cerium, zirconium, and hafnium, were selected as surrogates based on their thermodynamic properties and crystal

structure. The laser-synthesized samples were characterized by means of scanning electron microscopy (SEM), energy-dispersive X-ray spectroscopy (EDS) along with X-ray diffraction (XRD), where the different phases of formation, morphology, and microstructural features have been analyzed. Laser synthesis showed suitability for alloying Zr-Si and HfSi to ultimately form silicide compounds (Zr_3Si_2 and Hf_3Si_2).

In the study of Meng X.Y. et al. [24], to improve the performance and emission characteristics in the diesel/CNG dual-fuel combustion mode, bio-fuel of n-butanol as the additive in the pilot fuel was investigated by sweeping a wide range of CNG substitution rates.

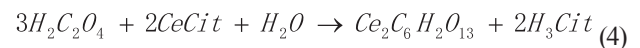
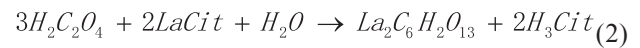
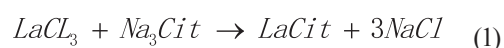
In the paper of Jamil A. [25], a basic solvothermal synthesis using sodium tungstate as a precursor is reported to prepare tungsten oxide (WO_3) particles. XRD data confirmed the highly crystalline nature. The broad peaks of XRD patterns estimated the nanocrystallites of WO_3 . The average crystallite size as was 95 nm. Scanning electron microscopy showed the morphologically cube-like particles with aggregation that was converted to larger brick-like particle of WO_3 after calcination. WO_3 was used as fuel additive in diesel oil. Fire and flash points of diesel oil were enhanced to 49 degrees C and 54 degrees C respectively. The calorific value was increased up to 36580 Jg(-1). Thus fuel efficiency was enhanced by use of WO_3 as an additive. The use of different concentrations of WO_3 (20, 40, 60, 80 ppm) as fuel additive has been also explored in this paper. The observed additive properties of WO_3 suggested the potential applications of such metal oxides.

In summary, although the research on fuel additives has made progress in stages, no one has been engaged in the research on organic rare earth as fuel additives for diesel engines. In order to solve the diesel engine exhaust gas to the environment pollution, organic acid rare earth fuel additives can be used to reduce NO_x , CO and HC emissions from internal combustion engines, in this study, the ability of La and Ce elements to store and release oxygen in organic complexes is used to improve combustion quality and reduce harmful gas emissions. This study adopts the method of theoretical analysis and experimental comparisons, finally an optimal formula of organic rare earth fuel additives can be found and put into practical application, it plays a guiding role in reducing exhaust gas pollution of diesel engine.

Materials and Methods

Preparation of the Fuel Additives of Lanthanum Oxalate and Cerium Oxalate

The reaction principle formula for preparing the lanthanum oxalate and cerium oxalate in this experiment is shown in Equations (1), (2), (3) and (4).



In the formula: Na_3Cit is Sodium citrate.

The specific preparation steps are as follows:

The same volume of ethanol and water is measured in the measuring cylinder, and 500 mL of the mixed solution is measured as the solvent of the reaction raw material after being evenly mixed in the agitator, and then transferred to the beaker for later use. The mass of the required raw materials is calculated. 0.1mol of lanthanum or cerium chloride hexahydrate ($LaCl_3 \cdot 6H_2O$ or $CeCl_3 \cdot 6H_2O$) is added to the mixed solution, followed by 0.08mol of sodium citrate ($Na_3Cit: C_6H_5Na_3O_7 \cdot 2H_2O$), magnetic stirring for 20 minutes, and then standing for 10 minutes. During this period, lanthanum or cerium citrate complex will be rapidly generated in the solution. Then 0.11mol oxalic acid ($H_2C_2O_4$) solution is dropped into the solution containing lanthanum or cerium citrate complex, stirred magnetically for 10 minutes, and then left standing. Lanthanum or cerium oxalate precipitates are gradually formed. After 24 hours of filtration and precipitation, the solution is washed twice with deionized water, washed again with anhydrous ethanol, and then dried at 80°C for 5 hours, the lanthanum or cerium oxalate powder can be prepared. Its molecular formula is $La_2C_6H_2O_{13}$ or $Ce_2C_6H_2O_{13}$.

Property Characterization of Fuel Additives

In order to study the emission reduction performance and internal relationship of fuel additives, the performance characterization of the fuel additives is carried out in the following steps.

X-ray Diffraction Analysis (XRD)

An appropriate amount of lanthanum and cerium oxalate powder is taken into the glass tank of the sample, evenly coated and pressed with a glass cover, and then placed in the X-ray diffractometer for experiment. The X-ray diffraction patterns obtained are shown in Fig. 1.

From the graph in Fig. 1a), we can see six distinct characteristic diffraction peaks with diffraction angles 2θ of 8.432°, 13.294°, 17.605°, 18.381°, 31.660° and 34.030° respectively.

After comparison and analysis with the standard card: product map was basically matched with JCPDS card (card No.00-049-1255; A = 11.378°, B = 9.631°, C = 10.497°), the space group showed as P21/C (14), and the diffraction peak could be confirmed as $La_2(C_2O_4)_3 \cdot 10H_2O$ monoclinic phase.

Apart from the influence of the instrument, the diffraction peak has a small degree of width, which may be caused by the small diameter of the sample

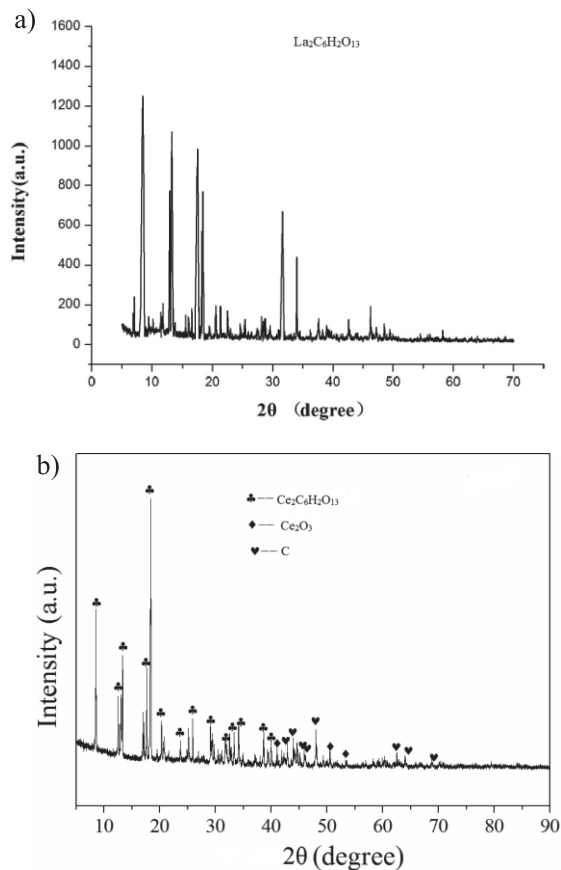


Fig. 1. XRD diagram of lanthanum and cerium oxalate powder: a) $\text{La}_2\text{C}_6\text{H}_2\text{O}_{13}$, b) $\text{Ce}_2\text{C}_6\text{H}_2\text{O}_{13}$.

particle and the refinement of the product. However, at the same time, many small hetero peaks are diffraction, which may be due to the entry of other elements when lanthanum ions combine with organic ligands, leading to the existence of other side reactions during preparation, or the vibration caused by instrument detection. XRD analysis showed that the additive was lanthanum oxalate with less impurity, and the preparation results were relatively successful.

From the graph in Fig. 1b), XRD diffraction pattern shows sharp and heterogeneous diffraction peaks. By comparison with standard PDF cards, it is found that it mainly corresponds to three phases $\text{Ce}_2\text{C}_6\text{H}_2\text{O}_{13}$, Ce_2O_3 , and C. The characteristic peak parameters of $\text{Ce}_2\text{C}_6\text{H}_2\text{O}_{13}$ completely match the phase of $\text{Ce}_2\text{C}_6\text{H}_2\text{O}_{13}$. It indicates that the preparation is successful. However, the diffraction peaks of Ce_2O_3 and carbon appear at the higher 2θ position, indicating the existence of some hybrid phases in the material.

Scanning Electron Microscope Analysis (SEM)

An appropriate amount of lanthanum and cerium oxalate powder is taken and dried in a drying oven at a constant temperature of 60°C for 1 hour before the scanning electron microscopy experiment is carried out. The samples are magnified 3000 times and photographed. The SEM photos are shown in Fig. 2.

From the graph in Fig. 2a), we can see that the powder of $\text{La}_2\text{C}_6\text{H}_2\text{O}_{13}$ presents a slender strip or dispersed granular, slender particles similar to the wormlike structure, may belong to the mesoporous structure. The particle diameter is in the range of 50-500 nm. While from the particle distribution, the distribution of small particles is more uniform, some large particles exist in the multi-layer distribution of particles. According to the SEM results, the fuel additive powder can be fully mixed with the fuel, which is conducive to the full combustion of the fuel to reduce the emission of NO_x , CO and HC.

From the graph in Fig. 2b), the preparation of cerium oxalate particles about 50-100 μm , it can be concluded that most of the particles disperse, the gap between the particles is obvious, no obvious particle agglomeration phenomenon. This is conducive to the full combination of oxygen and fuel in the combustion process, the whole is a dispersed crystal structure, the particle surface is smooth, no obvious impurity distribution, the material ratio of the preparation process is appropriate. However, some areas are suspected

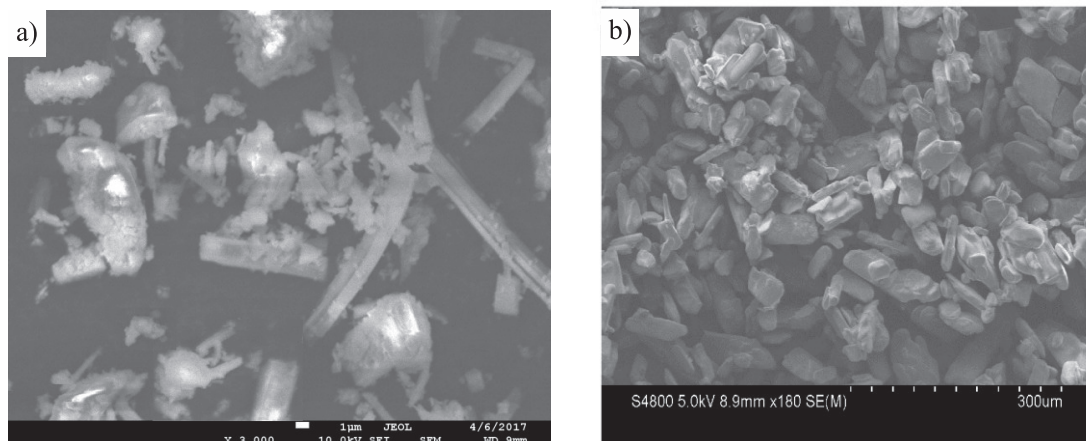


Fig. 2. SEM photo of lanthanum and cerium oxalate powder: a) $\text{La}_2\text{C}_6\text{H}_2\text{O}_{13}$, b) $\text{Ce}_2\text{C}_6\text{H}_2\text{O}_{13}$.

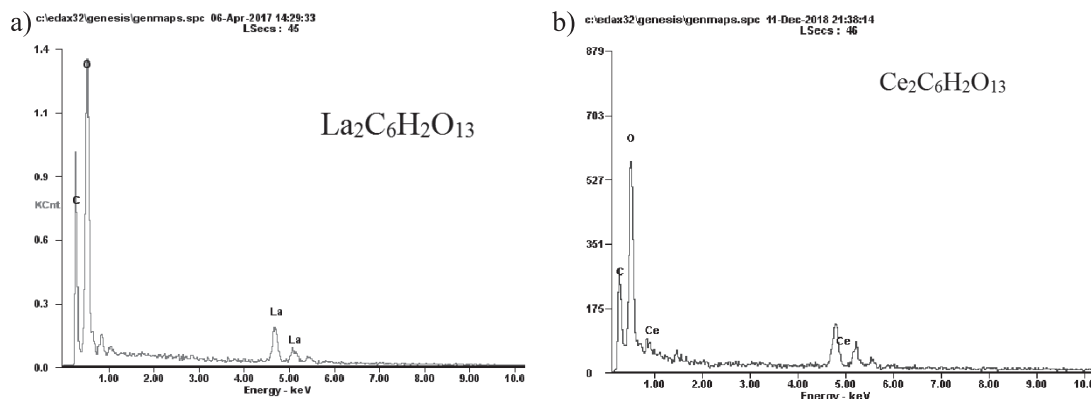


Fig. 3. EDS of lanthanum and cerium oxalate powder: a) $\text{La}_2\text{C}_6\text{H}_2\text{O}_{13}$, b) $\text{Ce}_2\text{C}_6\text{H}_2\text{O}_{13}$.

to be sintered. The stacking state of the particles is observed to be between 100-300 nm, and there are obvious particle contours at the junction. There is sintering phenomenon in the drying process of the preparation. It indicates that roasting time is too long, or some heat conduction in the solution is not uniform.

X-ray Scattering Energy Spectroscopy (EDS)

An appropriate sample powder surface was selected for X-ray irradiation, and the EDS energy spectrum analysis results were shown in Fig. 3 and Table 1.

According to the results in Fig. 3a) and Table 1, the main components of homemade lanthanum oxalate powder are elements C, O and La, and no other impurity elements appear in the sample without considering the element H. Similarly, the characteristic frequencies of K-line system and L-line system of La elements should be detected, and the characteristic peaks of the

two La elements should be displayed on the energy spectrum. The atomic number ratio of C, O and La in the energy spectrum table is 23.22:68.13:8.65, which is basically consistent with 6:13:2 of the chemical formula $\text{C}_6\text{H}_2\text{La}_2\text{O}_{13}$, in which the proportion of O element is increased. It is speculated that part of lanthanum oxalate may have been deliquesced during the preparation of the experimental sample. The percentage of atomic number of La element is 8.65%, and the less content is easy to disperse when it is decomposed at high temperature, so it is suitable for use as additive. Minor errors may be caused by different surface angles due to uneven powder distribution during testing or by test errors.

According to the results in Fig. 3b) and Table 2, the prepared cerium oxalate samples mainly compose of C element, O element, and Ce element. The atomic percentage in the table is 47.85:49.69:2.45, which is slightly different from that in cerium oxalate. By comparison, it can be observed that there is a proportion of O element, which may be caused by thermal decomposition reaction of some molecules in the process of drying decomposition, forming a small amount of CeO_2 solid, which has no influence on the dissolution of the main solvent.

Table 1. Element weight percentage and atomic number percentage of lanthanum oxalate.

Element	Wt%	At%
CK	10.84	23.22
OK	42.41	68.13
LaL	46.75	8.65
Matrix	Correction	ZAF

Table 2. Element weight percentage and atomic number percentage of cerium oxalate.

Element	Wt%	At%
CK	33.54	47.85
OK	46.40	49.69
CeL	20.06	2.45
Matrix	Correction	ZAF

Specific Surface Area Analysis (BET)

Nitrogen adsorption isotherm diagram of lanthanum oxalate powder is shown in Fig. 4.

As can be seen from Fig. 4a), the adsorption capacity of lanthanum oxalate increases slowly in the first half of the curve where the relative pressure (P/P_0) is relatively low. Then, in the middle of the curve, the adsorption amount has a rapid rising discontinuity, the curve shows a convex trend, and the adsorption is multi-layer adsorption under the relative pressure. The growth rate of the adsorption capacity decreases in the latter curve, which means that when the adsorption pressure is close to the saturated vapor pressure, the adsorption capacity will also have a tendency of saturation and will be less than a certain limit value, indicating that the pore size of lanthanum oxalate is limited.

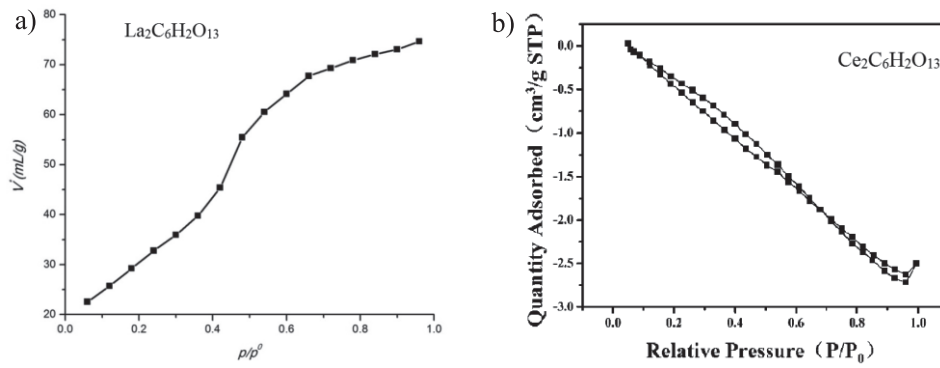


Fig. 4. Nitrogen adsorption isotherm diagram of lanthanum and cerium oxalate powder: a) $\text{La}_2\text{C}_6\text{H}_2\text{O}_{13}$, b) $\text{Ce}_2\text{C}_6\text{H}_2\text{O}_{13}$.

After the specific surface area analyzer was used to detect and calculate, the results obtained that the specific surface area of lanthanum oxalate sample was $92.85\text{m}^2/\text{g}$. Similarly, the self-made lanthanum oxalate powder has a relatively fine grain, and there are dense pores between each particle. In the cylinder, it can fully integrate with oil gas and participate in the combustion reaction, so as to achieve the ideal emission reduction effect.

As can be seen from Fig. 4b), the cerium oxalate isothermal adsorption curve belongs to the effective rising stage of type II isotherm. The inflexion point is not very obvious near the beginning, and it can be seen that the monolayer of cerium oxalate material completes slightly faster. Cerium oxalate has strong interaction with adsorbent in the convex direction of high P/P_0 curve, which shows a more obvious catalytic reaction during combustion. However, slight hysteresis and filling phenomenon can be seen in the middle and rear segments, indicating that the material begins to change into multi-molecule adsorption under this pressure. The back-end adsorption range remains at about $3.0\text{cm}^3/\text{g}$. The overall adsorption state increased steadily, and it is speculated that the emission reduction performance of the additive is stable after mixing with oil and gas. After the specific surface area analyzer was used to detect and calculate, the results obtained that the specific surface area of cerium oxalate sample was $102.85\text{m}^2/\text{g}$.

Results and Discussion

Changchai CZ2102 diesel engine is used in this experiment test. In the experiment test, 0# diesel oil is used as the base oil, and lanthanum or cerium oxalate fuel additives with additive mass fraction of 15 mg/L, 30 mg/L, 45 mg/L and 60 mg/L are added successively to make mixed fuel oil. Four kinds of mixed fuel oil are labeled as O15L, O30 L, O45L and O60L respectively. 0# diesel is denoted as O diesel. The mixed fuel is prepared on site before the test, and the dynamic characteristic test chart is drawn under different

rotating speeds, and the emission content is measured and compared at different working points.

On the diesel engine experiment, the main harmful emissions of the diesel engine are measured after the stable operation of the diesel engine for 15 minutes, and each working point is measured 3 times, and then the average value is taken to reduce the error.

In the diesel engine experiment test, the NO_x emission concentration of the dynamic characteristics of the five kinds of fuel oil is shown in Fig. 5, Fig.6, Table 3 and Table 4. As can be seen from the line chart, with the increase of diesel engine speed, NO_x emission concentration will increase, and the NO_x concentration curve value equipped with fuel additives

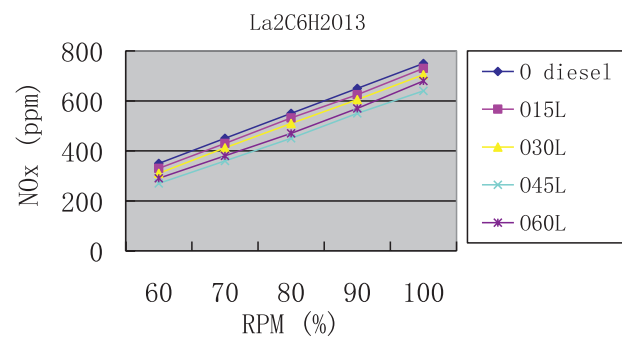


Fig. 5. NO_x emission concentration diagram of lanthanum oxalate fuel additives.

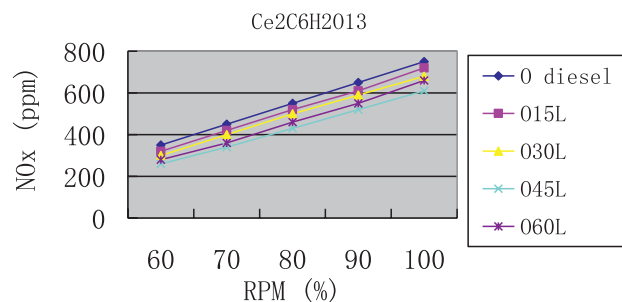


Fig. 6. NO_x emission concentration diagram of cerium oxalate fuel additives.

Table 3. NO_x emission concentration data of lanthanum oxalate fuel additives.

RPM (%)	60	70	80	90	100
O diesel	350	450	550	650	750
O15L	330	430	532	625	730
O30L	310	412	510	605	705
O45L	270	360	450	550	640
O60L	290	380	470	570	680
Max. Reduction (%)	22.8	20.0	18.2	15.4	14.7

Table 4. NO_x emission concentration data of cerium oxalate fuel additives.

RPM (%)	60	70	80	90	100
O diesel	350	450	550	650	750
O15L	320	420	520	610	720
O30L	300	400	500	590	680
O45L	260	340	430	520	610
O60L	280	360	460	550	660
Max. Reduction (%)	25.7	24.4	21.8	20.0	18.6

in the experiment test is below 0# diesel, and with the increase of additive content, the emission reduction effect is also significantly increased, O45L fuel oil of lanthanum oxalate can reduce the maximum NO_x emission by 22.8%, O45L fuel oil of cerium oxalate can reduce the maximum NO_x emission by 25.7%. It can be seen from the experiment that the use of lanthanum and cerium oxalate fuel additives has an obvious effect on reducing NO_x emission of diesel engine. However, as the speed increases, the emission reduction effect decreases.

In the diesel engine experiment test, the CO emission concentration of the dynamic characteristics of the five kinds of fuel oil is shown in Fig. 7, Fig. 8, Table 5 and Table 6. As can be seen from the line chart, with the increase of diesel engine speed, CO emission concentration will decrease, and the CO concentration curve value equipped with fuel additives

in the experiment test is below 0# diesel, and with the increase of additive content, the emission reduction effect is also significantly increased, O45L fuel oil of lanthanum oxalate can reduce the maximum CO emission by 39.4%, O45L fuel oil of cerium oxalate can reduce the maximum CO emission by 42.4%. It can be seen from the experiment that the use of lanthanum and cerium oxalate fuel additives has an obvious effect on reducing CO emission of diesel engine.

In the diesel engine experiment test, the HC emission concentration of the dynamic characteristics of the five kinds of fuel oil is shown in Fig. 9, Fig. 10, Table 7 and Table 8. As can be seen from the line chart, with the increase of diesel engine speed, HC emission concentration will decrease, and the HC concentration curve value equipped with fuel additives in the experiment test is below 0# diesel, and with the increase of additive content, the emission reduction

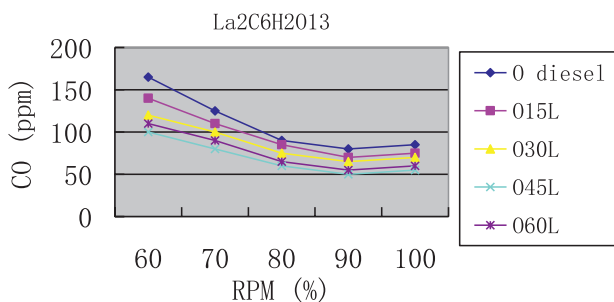


Fig. 7. CO emission concentration diagram of lanthanum oxalate fuel additives.

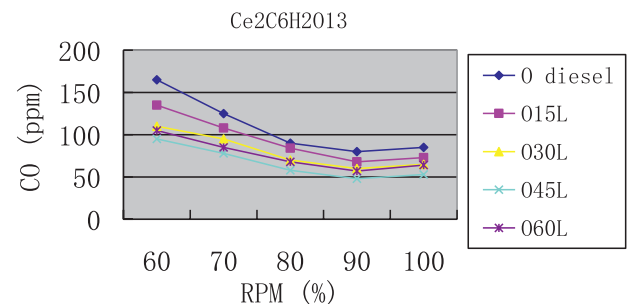


Fig. 8. CO emission concentration diagram of cerium oxalate fuel additives.

Table 5. CO emission concentration data of lanthanum oxalate fuel additives.

RPM (%)	60	70	80	90	100
O diesel	165	125	90	80	85
O15L	140	110	85	70	75
O30L	120	100	75	65	70
O45L	100	80	60	50	55
O60L	110	90	65	55	60
Max. Reduction (%)	39.4	36.0	33.3	37.5	35.3

Table 6. CO emission concentration data of cerium oxalate fuel additives.

RPM (%)	60	70	80	90	100
O diesel	165	125	90	80	85
O15L	135	108	84	68	73
O30L	110	95	70	60	65
O45L	95	78	58	48	53
O60L	105	85	68	57	64
Max. Reduction (%)	42.4	37.6	35.6	40.0	37.6

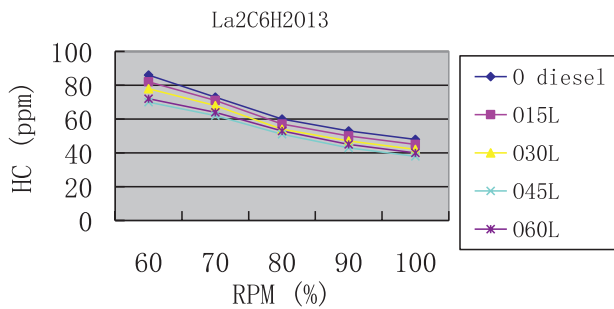


Fig. 9. HC emission concentration diagram of lanthanum oxalate fuel additives.

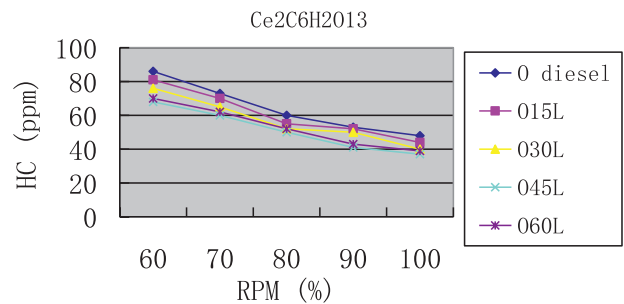


Fig. 10. HC emission concentration diagram of cerium oxalate fuel additives.

Table 7. HC emission concentration data of lanthanum oxalate fuel additives.

RPM (%)	60	70	80	90	100
O diesel	86	73	60	53	48
O15L	82	71	57	50	45
O30L	78	68	54	47	42
O45L	70	62	51	43	38
O60L	72	64	53	45	40
Max. Reduction (%)	18.6	15.1	15.0	18.9	20.8

effect is also significantly increased, O45L fuel oil of lanthanum oxalate can reduce the maximum HC emission by 20.8%, O45L fuel oil of cerium oxalate can reduce the maximum HC emission by 22.9%. It can be seen from the experiment that the use of lanthanum and

cerium oxalate fuel additives has an obvious effect on reducing HC emission of diesel engine.

In the diesel engine experiment test, PM emission concentrations of the dynamic characteristics of the five fuel oils are shown in Fig. 11, Fig. 12, Table 9 and

Table 8. HC emission concentration data of cerium oxalate fuel additives.

RPM (%)	60	70	80	90	100
O diesel	86	73	60	53	48
O15L	81	70	55	52	44
O30L	76	65	52	50	40
O45L	68	60	50	41	37
O60L	70	62	52	43	39
Max. Reduction (%)	20.9	17.8	16.7	22.6	22.9

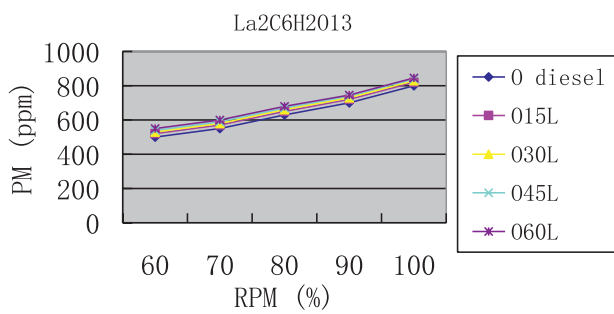


Fig. 11. PM emission concentration diagram of lanthanum oxalate fuel additives.

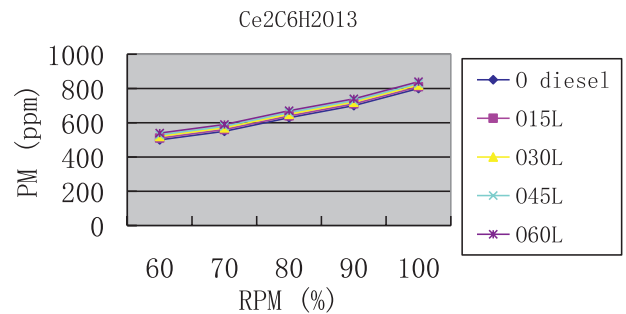


Fig. 12. PM emission concentration diagram of cerium oxalate fuel additives.

Table 9. PM emission concentration data of lanthanum oxalate fuel additives.

RPM (%)	60	70	80	90	100
O diesel	500	550	630	700	800
O15L	520	570	650	720	820
O30L	530	580	660	730	830
O45L	540	590	670	740	840
O60L	550	600	680	745	845
Max. Increase (%)	10.0	9.1	7.9	6.4	6.9

Table 10. PM emission concentration data of cerium oxalate fuel additives.

RPM (%)	60	70	80	90	100
O diesel	500	550	630	700	800
O15L	510	560	640	710	810
O30L	520	570	650	720	820
O45L	530	580	660	730	830
O60L	540	590	670	740	840
Max. Increase (%)	8.0	7.3	6.3	5.7	5.0

Table 10. As can be seen from the broken line chart, the PM concentration increases with the increase of diesel engine speed, and lanthanum and cerium oxalate fuel additive does not achieve the reduction effect in PM emission. During the whole experiment, compared with

0# diesel, the PM content of diesel engine equipped with fuel additive oil will increase to a certain extent, and the more the additive dose is added to the fuel oil, the higher the PM emission concentration will be. The maximum increment of PM emission concentration

is 10% when adding O60L. It can be seen from the experiment that PM increase of cerium oxalate fuel additives is less than that of lanthanum oxalate fuel additives.

According to the results of the experiment, why do NO_x, CO and HC decrease? Rare earth elements atomic structure is different from the other elements, the outermost is S2 structure, so the nature of rare earth metal elements are live, rare earth element La and Ce in oxygen storage are excellent performance, such as CeO₂ have strong ability of oxidation reduction, therefore cerium element +3 and +4 can be in conversion between two valence state, in the process of transformation of oxygen storage and release, when cerium switches between the +3 and +4 valence states the oxygen being produced increases the oxygen content of combustion, HC, CO and PM particles continue to be oxidized, NO_x continues to be reduced at the same time, so the harmful pollutants in the diesel engine exhaust gas can be reduced.

Why does PM increase? The reason is that although the fuel additives improve the combustion quality of fuel oil, the additives themselves are not completely burned, which causes a small increase in PM. The flammability of additives should be considered in the future research of additive emission reduction.

Conclusions

In the lanthanum oxalate powder, the content of La element is 8.65%, the particle diameter is in the range of 50-500nm, and the presence of mesoporous structure greatly increases the pore rate, and the specific surface area is detected to be 92.85m²/g.

In the cerium oxalate powder, the content of Ce element is 2.45%, the particle diameter is in the range of 100-300nm, and the presence of mesoporous structure greatly increases the pore rate, and the specific surface area is detected to be 102.85m²/g.

Finally, fuel additives of different concentrations are mixed with 0# diesel oil to produce some new mixed fuel oil, and the emissions of diesel engine are detected and analyzed. Then, the following conclusions are drawn:

1. NO_x emission of the lanthanum oxalate fuel additives decreased by 22.8%, NO_x emission of the cerium oxalate fuel additives decreased by 25.7%.
2. CO emission of the lanthanum oxalate fuel additives decreased by 39.4%, CO emission of the cerium oxalate fuel additives decreased by 42.4%.
3. HC emission of the lanthanum oxalate fuel additives decreased by 20.8%, HC emission of the cerium oxalate fuel additives decreased by 22.9%.
4. The maximum increment of PM emission of the lanthanum and cerium oxalate fuel additives is 10%.
5. The conclusion is that the lanthanum and cerium oxalate fuel additives with the mass fraction of about 45 mg/L is a more suitable choice. The results show that

reasonable use of lanthanum and cerium oxalate fuel additive can greatly reduce NO_x, CO and HC emissions from internal combustion engines.

6. Emission reduction effect of cerium oxalate fuel additive is better than that of lanthanum oxalate fuel additive. The results of their characteristic analysis are consistent with emission reduction effect of the two fuel additives.

Although the comparative study of lanthanum oxalate and cerium oxalate fuel additives is carried out in this study, their scope and experimental samples are small, and more emission reduction studies of organic acid rare earth fuel additives will be carried out in the future.

Data Availability

The data sets that support the findings of this study are available from the corresponding author upon a reasonable request.

Acknowledgments

In writing this paper, I have benefited from the presence of my colleagues. They generously helped me collect the materials I needed and made many invaluable suggestions. I hereby extend my grateful thanks to them for their kind help, without which the paper would not have been what it is.

Conflicts of Interest

The author declares that there is no conflict of interest regarding the publication of this paper.

Funding Statement

This work was supported by the National Natural Science Foundation of China. Grant number is 11272213.

References

1. ELSUNOUSI A.A.M., SEVIK H., CETIN M., OZEL H.B., OZEL H.U. Periodical and regional change of particulate matter and CO₂ concentration in Misurata. *Environmental Monitoring and Assessment*. **193** (11), **2021**.
2. CETIN M., ONAC A.K., SEVIK H., SEN B. Temporal and regional change of some air pollution parameters in Bursa. *Air Quality Atmosphere and Health*. **12** (3), 311, **2019**.
3. CETIN M. A Change in the Amount of CO₂ at the Center of the Examination Halls: Case Study of Turkey. *Studies on Ethno-Medicine*. **10** (2), 146, **2019**.

4. CETIN M., SEVIK H. Change of air quality in Kastamonu city in terms of particulate matter and CO₂ amount. *Oxidation Communications*. **39** (4), 3394, **2016**.
5. CETIN M., ALJAMA A.M.O., ALRABITI O.B.M., ADIGUZEL F., SEVIK H., CETIN I.Z. Determination and Mapping of Regional Change of Pb and Cr Pollution in Ankara City Center. *Water Air and Soil Pollution*. **233** (5), **2022**.
6. ZHANG C., MENG Z., CHEN C., WANG W., ZHANG J. Experimental research on the influence of iron base fuel additives on particulate emission in diesel engines. *Vehicle Engine*. **223** (2), 88, **2016**.
7. GONG J., LONG G., CAI H., WU G., YU M. Research on catalytic regeneration of particle traps based on ceri-based additives. *Journal of Internal Combustion Engine*. **29** (6), 5, **2011**.
8. JI Q., LIU Z., SUN P., WU Q., ZHAO S. Effects of nano fuel additives on particulate emission characteristics of diesel engines. *Vehicle Engine*. **5** (1), 64, **2015**.
9. MEI D., ZHAO X., WANG S., YUAN Y., SUN P. Thermo-gravimetric characteristics analysis of particulate matter of emission of divided diesel. *Transactions of the Chinese Society of Agricultural Engineering*. **29** (16), 50, **2013**.
10. SONG X., SONG D., DONG D., JIANG G., HUANG Z., CHEN Y. Experimental study on the influence of fuel additives on diesel emission of fishing boats. *Fishery Modernization*. **40** (6), 68, **2013**.
11. MA Z., WANG X., ZHANG X., PAN Y., XU B., WU J. Combustion and emission characteristics of pistacia seed biodiesel in diesel engine. *Journal of Internal Combustion Engine*. (05), 420, **2010**.
12. ZHANG D., DI Z., LIAN Y., YU J. Study on the preparation of nanoparticulate CeO₂ and its function as additive to improve fuel consumption and emission of diesel engine. *Petroleum Processing and Petrochemicals*. **42** (06), 66, **2011**.
13. WU Z., SUN P., MEI D., SUN Z., JI Y. Nano fuel additive CeO₂ to improve diesel combustion efficiency and reduce emissions. *Journal of Agricultural Engineering*. **29** (09), 64, **2013**.
14. WANG D., LIU Z., WANG Z., WU, N., LIU J. Influence of iron base fuel additives on diesel particulate emission. *Journal of Jilin University: Engineering Edition*. **42** (05), 1173, **2012**.
15. TIAN J., HAN Y., LIU Z., LI J., LI K. Performance and regeneration of the microprocessor after catalytic microparticles of diesel fuel. *Journal of Jilin University: Engineering Edition*. **41** (01), 18, **2011**.
16. DANILOV A.M. Research on Fuel Additives During 2011-2015. *Chemistry and Technology of Fuels and Oils*. **53** (05), 705, **2017**.
17. XIE Y., ZHANG J.S., BENSON M.T., KING J.A., MARIANI R.D. Assessment of Te as a U-Zr fuel additive to mitigate fuel-cladding chemical interactions. *Journal of Nuclear Materials*. **513**, 175, **2019**.
18. BENETT J. Additives for Spark Ignition and Compression Ignition engine fuels. *Proceedings of the Institution of Mechanical Engineers Part D-Journal Of Automobile Engineering*. **232** (1), 148, **2018**.
19. LARRSON E., OLANDER P., JACOBSON S. Boric acid as fuel additive - Friction experiments and reflections around its effect on fuel saving. *Tribology International*. **128**, 302, **2018**.
20. KESKIN A., YASAR A., YILDIZHAN S., ULUDAMAR E., EMEN F.M., KULCU N. Evaluation of diesel fuel-biodiesel blends with palladium and acetylferrocene based additives in a diesel engine. *Fuel*. **216**, 349, **2018**.
21. AKBARIAN E., NAJAFI B. A novel fuel containing glycerol triacetate additive, biodiesel and diesel blends to improve dual-fuelled diesel engines performance and exhaust emissions. *Fuel*. **236**, 666, **2019**.
22. SEZER I. Effect of nano materials additives on fuel properties and combustion characteristics. *Journal of the Faculty of Engineering and Architecture of Gazi University*. **34** (1), 115, **2019**.
23. ROSALES J., VAN ROOYEN I.J., PARGA C.J. Characterizing surrogates to develop an additive manufacturing process for U₃Si₂ nuclear fuel. *Journal of Nuclear Materials*. **518**, 117, **2019**.
24. MENG X.Y., ZHOU Y.H., YANG T.H., LONG W.Q., BI M.S., TIAN J.P., LEE C.F.F. An experimental investigation of a dual-fuel engine by using bio-fuel as the additive. **147**, 2238, **2020**.
25. JAMIL A. A novel study of tungsten oxide nanocrystallites as fuel additive for diesel oil. *Journal of Taibah University For Science*. **15**(1), 248, **2021**.